A Distributed Fixed-Time Secondary Controller for DC Microgrid Clusters

Sahoo, Subham; Mishra, Sukumar ; Fazeli, Seyed; Li, Furong; Dragicevic, Tomislav

Published in:
I E E E Transactions on Energy Conversion

DOI (link to publication from Publisher):
10.1109/TEC.2019.2934905

Publication date:
2019

Document Version
Accepted author manuscript, peer reviewed version

A Distributed Fixed-Time Secondary Controller for DC Microgrid Clusters

Subham Sahoo, *Member, IEEE*, Sukumar Mishra, *Senior Member, IEEE*, Seyed Mahdi Fazeli, Furong Li, *Senior Member, IEEE* and Tomislav Dragičević, *Senior Member, IEEE*

***Abstract*—In realistic scenarios, the dynamic performance of a microgrid cluster is largely affected by the intermittent power of renewable energy sources and frequent load changes. To address this issue, a distributed fixed-time based dual layer secondary controller is designed to improve inter-microgrid and intra-microgrid dynamic performance within a fixed settling time. The proposed controller is independent of initial operating values as opposed to the finite time control law. Each global agent in a microgrid operates to mitigate loading mismatch between other global agents, whereas each local agent in a microgrid operates to achieve proportionate load current sharing and average voltage regulation between them in fixed time. However, as loading mismatch mitigation during light load conditions affects the system efficiency due to significant line losses, the cluster operation switches to a distributed loss minimization approach, which operates using online measurements from the neighboring microgrids. To characterize the mode of operation in the global cyber layer, a critical point of loading threshold for the cluster is thus determined. The performance of the cluster employing the proposed strategy is simulated in MATLAB/SIMULINK environment for various scenarios to demonstrate its reliability and efficiency.**

***Index Terms*—DC microgrid clusters, cooperative control, fixed-time consensus, secondary control.**

I. Introduction

DC microgrids are effective means of integrating renewable energy sources, storage devices and modern electronic loads, capable of operating independently of the utility grid [1]- [2]. Additional features include characteristics such as improved reliability [3] and scalability [4]. Further research also suggests that autonomous operation in DC paradigm results in improved efficiency by avoiding power exchange with the grid [5]. This also leads to a reduction in the number of conversion stages without resorting to synchronization, power quality issues in the AC counterparts.

To alleviate the scope of enhancing balanced utilization of their sources in autonomous mode, multiple DC microgrids are usually interconnected to form a cluster. Proper coordination among distributed sources in a cluster plays an increasingly important role as it directly affects the system performance [6]. To address this concern, secondary controllers are usually employed to compensate for the drift caused by the local primary controllers and line impedance mismatches [7]. The secondary control philosophy usually requires communication as it is based on measurements from the participating units, commonly termed as *agents*. To accommodate these changes, centralized communication is usually carried out due to its simple two-way structure which involves the transmission of signals from each agent to a central controller and vice-versa. However, it affects system reliability owing to its vulnerability to a single-point-of-failure [8]. Alternatively, distributed communication [10] provides an economic, scalable platform for the neighboring agents to reach consensus thereby establishing system stability.

Using distributed cyber topology, significant research has been conducted for DC microgrids, which involves proportionate load sharing, average voltage regulation and energy balancing such that the utilization factor of the sources is always balanced [11], [12]. However, the above-mentioned studies have been carried out in unrealistic fashion because desired current sharing profile is always assumed to be proportional. In sharp contrast, realistic systems exhibit frequent load changes and intermittent power availability from renewable energy sources. Moreover, this effect is specifically pronounced in a cluster of microgrids where there are multiple nodes with intermittent sources and loads. In [13], the authors have proposed a two-layer distributed tertiary controller to mitigate loading mismatch between DC microgrids in a cluster, which is based on the philosophy of voltage adjustment policy using the pinning link concept. However, this strategy focuses primarily on asymptotic convergence which can have adverse effects on the network performance during frequent disturbances.

To address this issue, a finite-time synchronization concept in DC microgrids is proposed by Sahoo, *et. al.* in [4] which features convergence of states within a finite bounded time having ensured stable performance. However, finite-time schemes highly depend on initial operating conditions, which may not always be available. On the other hand, it becomes a complicated task to realize finite-time consensus in a large system where the state dynamics may depend on multiple variables.

By analysis, to maximize utilization of renewable energy sources, mitigating loading mismatch between microgrids is a prevalent option regardless of how they are dynamically coupled [14]. As a result of this approach during light loading conditions, the transmission line losses become significant

This work was supported by the DST, Government of India under project "Identification and Demonstration of Cost Effective Technologies to Maximize Habitat Energy Self-sufficiency" with file no. TMD/CERI/BEE/2016/096(G).

S Sahoo and T Dragičević are with the Department of Energy Technology, Aalborg University, Aalborg East 9220, Denmark (e-mail: sssa@et.aau.dk and tdr@et.aau.dk)

S Mishra is with the Department of Electrical Engineering, Indian Institute of Technology Delhi, New Delhi 110 016, India. (e-mail: sukumar@ee.iitd.ac.in)

SM Fazeli and F Li are with the Department of Electronic & Electrical Engineering, University of Bath, UK. (e-mail: S.M.Fazeli@bath.ac.uk and F.Li@bath.ac.uk)

as compared to the converter losses [16]. Many approaches have been considered in order to improve the efficiency by enhancing converter performance [17], stability assessment with variable droop [18], etc. Moreover, the design of such strategies are often carried out in a centralized fashion where each update is received after a prolonged time-scale, thereby categorizing them as a tertiary update.

These issues are addressed for the first time in this paper, which proposes a fixed-time based dual layer distributed controller to maintain cluster coordination at both global and local level within fixed settling time. The significance behind using fixed-time consensus for cluster synchronization is that it guarantees an upper bound on the settling time, independent of initial operating values. To address the second problem, a fully distributed optimal update for loss minimization is obtained within fixed-time to alleviate system efficiency during light load conditions. Since loss minimization and mitigating loading mismatch can not take place simultaneously, the traversal of the mode of cluster operation in the global layer is anticipated by determining a minimum tie-line current threshold above which loading mismatch mitigation is used for the global secondary controller.

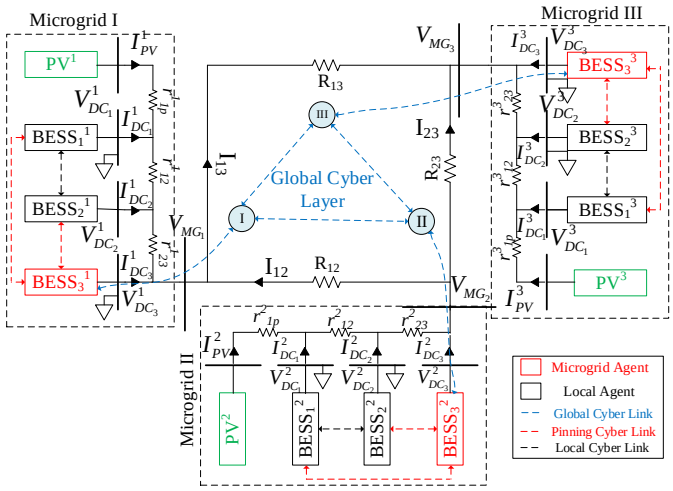

Fig. 1. Single-line diagram of the modeled DC microgrid cluster with dual cyber layer communication.

To sum up, the research contributions of this paper are:

1) A global layer fixed-time based cooperative secondary controller to mitigate the loading mismatch between microgrids using microgrid agents in a cluster within fixed settling time. The advantage behind using fixed-time consensus theory is that it is independent of their initial conditions, which may be unknown in many cases for large systems, thus making it a practical approach.
2) A cooperative loss minimization update using distributed optimization is obtained within fixed-time to enhance system efficiency only during the light load conditions. A critical point of loading threshold is determined which characterizes the mode traversal between loss minimization and loading mismatch mitigation.
3) A local layer fixed-time based cooperative secondary controller to manage proportionate load current sharing maintaining average voltage regulation in each microgrid within fixed time. Further, a pinning gain concept is used to broadcast the global information into the local nodes.

The rest of the paper is organized as follows. Section II presents the cyber-physical DC microgrid cluster with a brief overview of the conventional cooperative techniques and control objectives. Section III depicts the proposed control strategy involving both layers of communication. The stability of the proposed controller is carried out in Section IV along with a time-delay based stability analysis under different communication delay. The performance of the proposed control strategy under various disturbances has been evaluated in Section V. Finally, Section VI concludes the paper.

II. Cyber-physical DC Microgrid Clusters

Fig. 1 shows a single-line diagram of the modeled cluster with M=3 DC microgrids, each consisting of N=3 battery storage devices, a PV farm and loads. It is worth mentioning that each battery energy storage system (BESS) is connected to the DC bus through a DC/DC bidirectional converter used to regulate the output voltage. On the other hand, PV is connected to the DC bus via a DC/DC boost converter. It should be noted that k^{th} agent in c^{th} microgrid as shown in Fig. 1 is connected to j^{th} agent via resistive tie-lines of r^c_{kj}. Furthermore in the cluster, c^{th} microgrid is connected to the m^{th} microgrid via a tie-line resistance of R_{cm} to form a *cluster* of microgrids as shown in Fig. 1. The local layer of communication in each microgrid, highlighted as black dotted lines with arrows in Fig. 1, is used for fixed-time based cooperative control to achieve proportionate load current sharing and average voltage regulation using neighboring measurements within a microgrid. Similarly, the global layer of communication between microgrids, highlighted as blue dotted lines in Fig. 1, allows mitigation of loading mismatch between them using fixed-time consensus theory in the cluster. To achieve coordination between both layers, the microgrid agents in the global layer are pinned to local agents via pinning link, highlighted as red dotted lines with arrows in Fig. 1, to broadcast global response in each microgrid. Since this paper is solely based on voltage control at each bus, BESSs are represented as *agents* corresponding to every node in the cyber graph. It is worth notifying that PV is not considered as an agent since it acts as a current source, which always operates at MPPT.

The global layer adjacency matrix $\tilde{A} = [a^{cm}]\ \epsilon\ R^{MXM}$ via edges and links can be mathematically represented as:

$$a^{cm} = \begin{cases} > 0, & \text{if } (x^c, x^m)\ \epsilon\ \tilde{\Xi} \\ 0, & \text{else} \end{cases} \tag{1}$$

where a^{cm}, x^c, x^m and $\tilde{\Xi}$ represent the adjacency matrix weights for cyber links, parent microgrid agent, neighboring microgrid agent in a cluster and the set of edges in the global layer respectively for the neighboring set of microgrids for c^{th} microgrid, denoted as N_c.

To replicate the response from the global level in each microgrid, the microgrid agents communicate to the pinned agents of their respective microgrid as shown in Fig. 1. Further, the pinned agent in each microgrid forms a local distributed

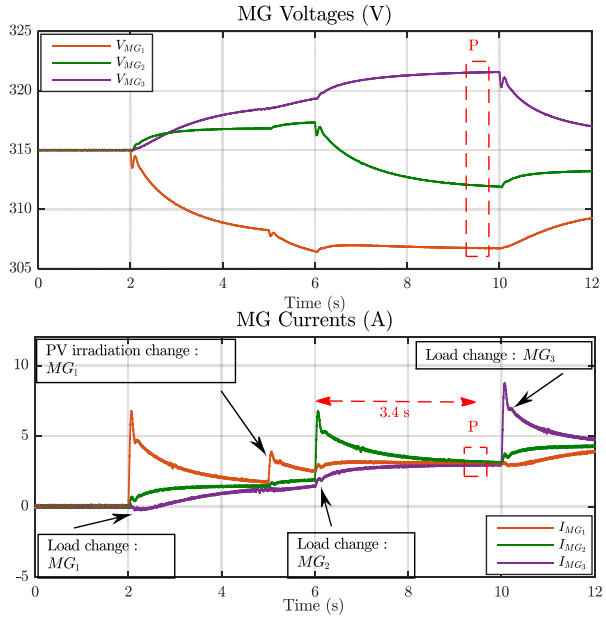

Fig. 2. Performance of conventional distributed tertiary controller [13]: Asymptotic convergence causing slow current sharing & voltage restoration.

channel wherein each local agent sends and receives information from its neighbors. Representing the digraph via edges and links using an adjacency matrix $A_c = [a^c_{kj}] \; \epsilon \; R^{NXN}$ with the communication weights to be:

$$a^c_{kj} = \begin{cases} > 0, & \text{if } (x^c_k, x^c_j) \; \epsilon \; E \\ 0, & \text{else} \end{cases} \tag{2}$$

where E is an edge connecting two nodes, x^c_k is the parent local agent, x^c_j is the neighboring local agent in c^{th} microgrid and N^c_k denote the set of neighboring agents of k^{th} agent in c^{th} microgrid.

To realize the secondary control objectives in [11] and tertiary input on loading mismatch mitigation in [13], the control laws are designed in such a manner so that:

$$\lim_{t\to\infty} |\bar{V}^c_{DC_j}(t) - \bar{V}^c_{DC_k}(t)| = 0 \tag{3}$$

$$\lim_{t\to\infty} |I^c_{DC_j}(t) - I^c_{DC_k}(t)| = 0 \tag{4}$$

$$\lim_{t\to\infty} |I_{MG_m}(t) - I_{MG_c}(t)| = 0 \tag{5}$$

where $\bar{V}^c_{DC_k}$ and $I^c_{DC_k}$ represent the average voltage and BESS current of k^{th} (parent) agent in c^{th} microgrid respectively. It should be noted that V_{MG_c} in Fig. 1 represent the voltage bus of each microgrid, which is physically close to the microgrid agent. Moreover, I_{MG_c} represents the microgrid current which corresponds to available generation/load at rated voltage in c^{th} microgrid, which is given by:

$$I_{MG_c}(t) = I^c_{PV}(t) - I^c_L(t) \tag{6}$$

where I^c_{PV} and I^c_L denote the PV and local load current in c^{th} microgrid respectively. (6) will always hold true since BESSs are operating in voltage controlled mode.

Since the objectives in (3)-(5) have been achieved in an asymptotic manner where the error converges typically in seconds [13], a dual layer fixed-time based cooperative secondary controller is proposed in this paper which is described in the next section.

To provide a clear picture of the performance issues caused by conventional distributed tertiary controller [13] operating to achieve (3)-(5) in a cluster, a case study is considered in Fig. 2 for the modeled cluster in Fig. 1 where disturbances such as load change and PV irradiation change are introduced frequently. It can be seen in Fig. 2 that for load changes at t = 2 and 5 s, loading mismatch error between microgrids hasn't reduced to zero causing a reduction in energy efficiency due to momentary increase in generation cost. Moreover, the voltages at each microgrid bus haven't settled thereby affecting the network performance. To reach a steady state error of zero (at point P), it takes around 3.4 s which doesn't justify for compelling performance due to frequent disturbances in a cluster.

III. Proposed Fixed-Time Control Strategy

A. Inter-Microgrid Objectives

The general objective of the proposed strategy in the global layer switches between loss minimization during light load conditions & loading mismatch mitigation to improve system efficiency. The losses in a cluster can typically be categorized into transmission loss and power conversion losses in DC/DC converter such as switching and conduction losses. As the authors in [19] have reported that converter efficiency varies under different loading conditions, loading mismatch mitigation between microgrids reduce system efficiency as the transmission line ($R_{cm} >> r^c_{kj}$) losses between microgrids become high as compared to the conversion losses. This necessitates a loss minimization approach to be carried out during light load conditions.

1) Loss Minimization: To implement this strategy, a critical point of loading level needs to be determined to introduce mode traversal between loss minimization & loading mismatch mitigation. Considering the efficiency curves for each converter at different loading levels, the critical point of loading can be analyzed. This aspect has been discussed in detail in the following section. Formulating the inter-microgrid objectives based on the above criteria, the global secondary controller is alternatively run in two modes using a signal:

$$\phi = \begin{cases} 0, \text{if } \sum_{i=1}^{N} I_{MG_c} \leq \kappa I_{cap} \\ 1, \text{else} \end{cases} \tag{7}$$

where the threshold of κ (in p.u.) of full load (I_{cap}) is considered for mode switching of global operation in the modeled system operating at their rated voltages. The transmission line losses are minimized using the objective function:

$$\textbf{min} \sum_{c,m\epsilon M} C_{cm}(I_{cm}) = I^2_{cm} R_{cm} \tag{8}$$

where I_{cm} denote the tie-line current between c^{th} & m^{th} microgrid. In other words, minimization of (8) will be achieved when:

$$\sum_{c,m\epsilon M} \lambda_{cm} = \sum_{c,m\epsilon M} \frac{dC_{cm}}{dI_{cm}} = \sum_{c,m\epsilon M} 2 I_{cm} R_{cm} \to 0 \tag{9}$$

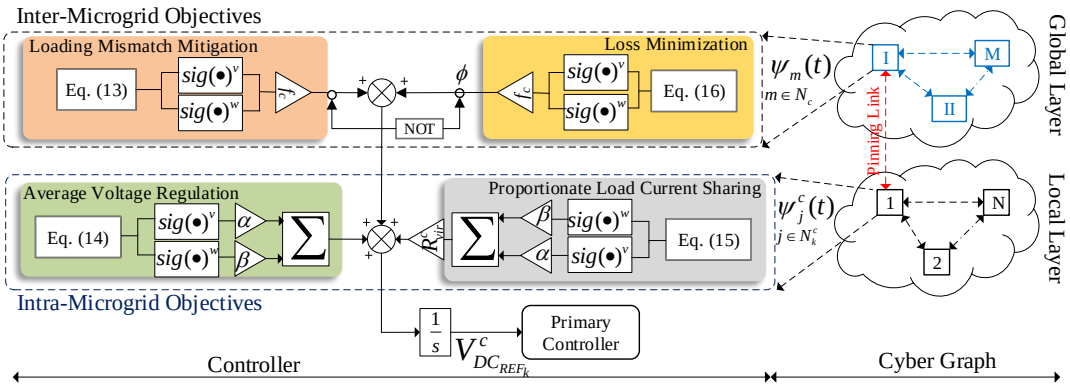

Fig. 3. Proposed control strategy for the pinned agent in c^{th} microgrid

where λ_{cm} is an online iterative factor for loss minimization. Moreover, (8) is solved with the decision variable as $[I_{cm}]\ \forall\ c, m\ \epsilon\ M$, subject to

TABLE I
PROPOSED CONTROL PHILOSOPHY IN THE CLUSTER

ϕ	Inter-Microgrid Objectives	Intra-Microgrid Objectives
0	Loss Minimization	Average Voltage Regulation; Proportionate Load Current Sharing
1	Loading Mismatch Mitigation	Average Voltage Regulation; Proportionate Load Current Sharing

$$I_{cm}^{min} < I_{cm} < I_{cm}^{max} \tag{10}$$

$$\sum I_{cm} = I_{load}\ \forall\ c, m = 1, .., M \tag{11}$$

for a load current given by:

$$I_{load} = \begin{cases} \sum_{c\epsilon M} I_{MG_i}, \text{if } I_{MG_c} > 0 \\ 0, \text{else} \end{cases} \tag{12}$$

where I_{ij}^{min} and I_{ij}^{max} denote minimum and maximum value of tie-line current respectively. It is worth mentioning that I_{ij}^{min} and I_{ij}^{max} are calculated by adding the current generation from PV and minimum and maximum capacity of bidirectional converter respectively. Hence, a modified set of inter-microgrid objectives for DC microgrid clusters is presented in this paper to improve system efficiency as compared to [13].

2) Loading Mismatch Mitigation: To mitigate loading mismatch between micrigrids across the cluster, using the intra-microgrid sharing objectives suggesting proportionate load current sharing with known value of N agents in c^{th} microgrid, I_{MG_c} for loading mismatch mitigation can be found out using $I_{MG_c} = NI_{DC_k}^c$, where $I_{DC_k}^c$ depict the output current from the microgrid agent of c^{th} microgrid. Hence, loading mismatch mitigation is achieved using the following input:

$$\dot{I}_{MG_c}(t) = \underbrace{\sum_{m\epsilon N^c} \underbrace{I_{MG_m}(t) - I_{MG_c}(t)}_{e_{k_1}^c(t)}}_{u_{I_{MG}}^c(t)} = 0. \tag{13}$$

It is worth notifying that the intra-microgrid objectives are always operating simultaneously with inter-microgrid objectives in the cluster, as shown in Table I. However, the mode of operation in inter-microgrid objectives, i.e. either loss minimization or loading mismatch mitigation, is traversed using (7) based on the loading condition.

B. Intra-Microgrid Objectives

In the local layer, the local agents cooperate to carry out average voltage regulation as well as proportionate load current sharing simultaneously in their respective microgrids. More details on these objectives in DC microgrids can be referred from [4]. In order to estimate average voltage, a distributed voltage observer is employed using *dynamic consensus* [11] of agents. The average voltage estimate $\bar{V}_{DC_k}^c$ in c^{th} microgrid for k^{th} agent is given by:

$$\dot{\bar{V}}_{DC_k}^c(t) = \dot{V}_{dc_k}^c(t) + u_{V_k}^c(t) \tag{14}$$

where $u_{V_k}^c(t) = \sum_{j\epsilon N_k^c} a_{kj}^c \underbrace{(\bar{V}_{DC_j}^c(t) - \bar{V}_{DC_k}^c(t))}_{e_{k_2}^c(t)}$. Similarly, the load current in c_{th} microgrid is shared by using:

$$\dot{I}_{DC_k}^c(t) = \underbrace{d_i \sum_{j\epsilon N_k^c} a_{kj}^c \underbrace{(I_{DC_j}^c(t)/I_{DC_j}^{c,max} - I_{DC_k}^c(t)/I_{DC_k}^{c,max})}_{e_{k_3}^c(t)}}_{u_{I_k}^c(t)} = 0 \tag{15}$$

where d_i denotes a positive coupling gain. Assembling all the control inputs from (9), (13)-(15), the fixed-time consensus is formulated for the cluster in the following subsection.

C. Design of Fixed-Time Controller

The design of a fixed-time based distributed secondary controller is discussed in this section. Further details & formulation for fixed-time stability is given in [21]. Using (9), a distributed update for loss minimization λ_c for c^{th} microgrid is given by:

$$\dot{\lambda}_c = \underbrace{h_c \sum_{o,z\epsilon N_c} \underbrace{(\lambda_{oz} - \lambda_{cm})}_{e_{k_4}^c(t)}}_{u_\lambda^c} = 0 \tag{16}$$

where h_c serves as a coupling gain to denote (16) in terms of a voltage correction update for the controller.

To sum up, the errors defined as per the proposed strategy for the cluster are merged into a matrix $E_k^c = \{e_{k_1}^c, e_{k_2}^c, e_{k_3}^c, e_{k_4}^c\}$ undergo fixed-time consensus such that:

$$\lim_{t \to T^*} |E_m^c(t) - E_k^c(t)| = 0, \ \forall \ m \ \epsilon \ N_c \tag{17}$$

where T^* is the upper bound on the fixed time required for

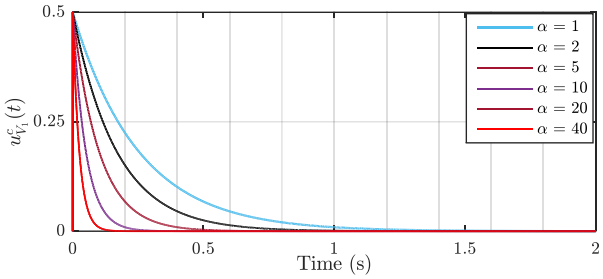

Fig. 4. Performance evaluation of fixed-time convergence of the proposed strategy with different values of α for β = 3: Increase in α results in faster settling time.

convergence. To implement (17), all the control inputs defined above are used in (14) to get the fixed-time voltage control input as:

$$\begin{aligned} \dot{\hat{V}}_{DC_k}^c(t) \quad = \quad & \dot{V}_{DC_k}^c(t) + \alpha sig^v u_{V_k}^c(t) + \phi f_c sig^v u_{I_{MG}}^c(t) \\ & + (1-\phi) f_c sig^v u_\lambda^c + \beta sig^w u_{V_k}^c(t) + \\ & \phi f_c sig^w u_{I_{MG}}^c(t) + (1-\phi) f_c sig^w u_\lambda^c \end{aligned} \tag{18}$$

where $0> \ v \ >1$, $0> \ w \ >1$, $\alpha \ > \ 0$, $\beta \ > \ 0$, $sig^a(x) = sig(x)|x|^a$ with $sig(\circ)$ denoting sign function and f_c denote the pinning gain matrix. Similarly, the fixed-time current control input from (15) is given by:

$$\dot{I}_{DC_k}^c(t) \quad = \quad \alpha sig^v u_{I_k}^c(t) + \beta sig^w u_{I_k}^c(t). \tag{19}$$

Using the primary control law for DC microgrids [4], the final voltage reference $V_{DC_{REF_k}}^c$ for fixed-time stability is given by:

$$V_{DC_{REF_k}}^c = \int (\dot{V}_{DC_k}^c + R_{vir} \dot{I}_{DC_k}^c) \tag{20}$$

which is used in the primary controller of k^{th} agent in c^{th} microgrid, as shown in Fig. 3. These control functions are achieved using local as well as neighboring measurements, given by:

$$\psi_m(t) = \{I_{MG_m}, \lambda_{oz}\}, \ m, o, z \ \epsilon N_c \tag{21}$$

$$\psi_j^c(t) = \{I_{DC_j}^c, V_{DC_j}^c, \bar{V}_{DC_j}^c\}, \ j \ \epsilon N_k^c \tag{22}$$

where $\psi_m(t)$ and ψ_j^c depict the neighboring measurements in global and local layer as highlighted in Fig. 3 respectively. It is worth notifying that the fixed-time convergence is a bounded phenomena and operates within physical converter current limit, which is already considered in the inner current control loop of the bidirectional control strategy of each agent.

D. Performance Evaluation

The convergence speed of the proposed fixed-time strategy is monitored for different values of the design gains α and β. As it can be seen in Fig. 4, the convergence speed of $u_{V_1}^c(t)$

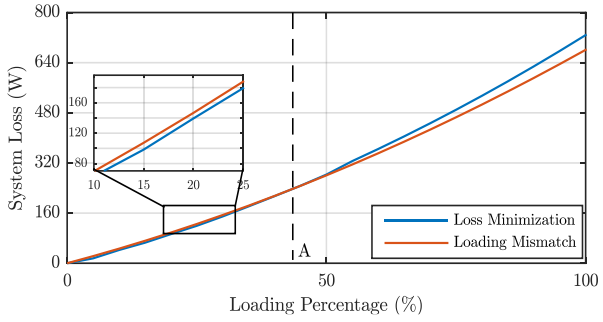

Fig. 5. System loss at different load levels: Point A determines the critical point for mode traversal in global objectives in (7).

increases with increase in the value of α for a constant value of β = 3. However, these gains can't be incessantly increased considering different communication sampling rate of each cyber layer which indirectly limits the dynamic performance of the controller. Taking this into consideration, design guidelines of these gains with respect to the communication sampling rate is provided in Appendix B.

To identify the threshold for switching the mode of operation in (7), the system efficiency in microgrid level needs to be monitored for different loading levels in the cluster. It should be noted that this analysis is model-dependent, and relies on parameters such as line parameters, size and converter efficiencies, etc. More details can be referred from [19]. Considering the modeled system in Fig. 1 and converter efficiencies in [10] for a maximum load of 16 kW, it can be seen in Fig. 5 that the system loss is lower when operated with loss minimization approach as compared to the loading mismatch mitigation strategy for loading level below point A and vice-versa. Moreover, the value of κ in (7), corresponds to point A in Fig. 5, which is around 42 % of the maximum loading in the modeled system. It is worth mentioning that a dwell time of 1 sec is used in the proposed control strategy to avoid chattering between two modes in (7). Hence, the mode traversal between both the inter-microgrid objectives based on the condition in (7) for efficient operation of any system can be supervised in this manner. The stability of the proposed controller is carried out in the following section to distinguish fixed-time from finite-time control strategy.

IV. Stability Analysis

In this section, the stability of the proposed controller for the modeled system is investigated considering each error dynamics, the Lyapunov candidate $V(t)$ is defined as:

$$V(t) \quad = \quad \frac{1}{2} \sum_{c=1}^{M} \sum_{k=1}^{N} E_k^c(t)^T E_k^c(t) \tag{23}$$

Differentiating (23), we split the candidates into $V_1(t) - V_5(t)$, given by:

$$\begin{aligned}\dot{V}(t) &= \underbrace{\sum_{c=1}^{M}\sum_{k=1}^{N} E_k^c(t)^T f(E_k^c(t))}_{V_1(t)} + \\ &\underbrace{+\alpha\sum_{c=1}^{M}\sum_{k=1}^{N} E_k^c(t)^T \sum_{j\epsilon N_k^c} a_{kj}^c sig^v(E_j^c(t) - E_k^c(t))}_{V_2(t)} \\ &\underbrace{+\sum_{c=1}^{M}\sum_{k=1}^{N} E_k^c(t)^T \sum_{j\epsilon N_c} sig^v \sum_{j\epsilon N_k^c} a_{kj}^c E_j^c(t)}_{V_3(t)} \\ &\underbrace{+\beta\sum_{c=1}^{M}\sum_{k=1}^{N} E_k^c(t)^T \sum_{j\epsilon N_k^c} a_{kj}^c sig^w(E_j^c(t) - E_k^c(t))}_{V_4(t)} \\ &\underbrace{+\sum_{c=1}^{M}\sum_{k=1}^{N} E_k^c(t)^T \sum_{j\epsilon N_c} sig^w \sum_{j\epsilon N_k^c} a_{kj}^c E_j^c(t)}_{V_5(t)} \end{aligned} \quad (24)$$

where $f(\circ) = sig^v(\circ)$ is a QUAD function, which is used to calculate the area under two distinct points. This suggests that for a positive value of σ,

$$(x_1 - x_2)^T(f(x_1) - f(x_2) \leq \sigma(x_1 - x_2)^T(x_1 - x_2) \quad (25)$$

holds true. Using (25), we get $V_1(t) \leq 2\sigma V(t)$. Moreover, since $a_{kj}^c = a_{jk}^c$ and $sig^v(E_j^c(t) - E_k^c(t)) = -sig^v(E_k^c(t) - E_j^c(t))$, $V_2(t)$ can be simplified as:

$$\begin{aligned} V_2(t) &= -\frac{\alpha}{2}\sum_{c=1}^{M}\sum_{k=1}^{N}\sum_{j\epsilon N_k^c} a_{kj}^c |E_j^c(t) - E_k^c(t)|^{1+v} \quad (26) \\ &\leq -\frac{\alpha}{2}[\sum_{c=1}^{M}\sum_{k=1}^{N}\sum_{j\epsilon N_k^c} (a_{kj}^c)^{\frac{2}{1+v}} |E_j^c(t) - E_k^c(t)|^2]^{\frac{1+v}{2}} \\ &\leq -\frac{\alpha}{2}[2\sum_{k=1}^{N} \xi_2(-\bar{A}_{ll}^c) E_k^c(t)^T E_k^c(t)]^{\frac{1+v}{2}} \\ &\leq -\frac{\alpha}{2}[4\rho V(t)]^{\frac{1+v}{2}} = -\Gamma_1 V(t)^{\frac{1+v}{2}} \quad (27) \end{aligned}$$

where $\bar{A}_{ll}^c$=$[\bar{a}_{kj}^c]$ ϵ R^{NXN}, such that the communication weights are given by:

$$\bar{a}_{kj}^c = \begin{cases} (a_{kj})^{\frac{2}{1+v}}, \text{ if } k \neq j \\ -\sum_{k,j\epsilon N}(a_{kj})^{\frac{2}{1+v}}, \text{ else} \end{cases} \quad (28)$$

Moreover, ρ_1 denote the minimum eigenvalue of $\bar{A}_{ll}^c$ and $\Gamma_1 = \alpha 2^v \rho^{\frac{1+v}{2}}$. On the other hand,

$$\begin{aligned} V_3(t) &\leq \sum_{c=1}^{M}\sum_{k=1}^{N}\sum_{j\epsilon N_c} |E_k^c(t)|^T |\sum_{j\epsilon N_k^c} a_{kj}^c E_j^c(t)| \quad (29) \\ &= a_{max}^v \sum_{c=1}^{M}\sum_{k=1}^{N} |E_k^c(t)|^{1+v}[N - (r_c - r_{c-1})] \\ &\leq a_{max}^v \bar{r} \sum_{c=1}^{M}\sum_{k=1}^{N} (|E_k^c(t)|^2)^{\frac{1+v}{2}} \\ &\leq a_{max}^v \bar{r}(N)^{\frac{1-v}{2}} [\sum_{c=1}^{M}\sum_{k=1}^{N} (|E_k^c(t)|^2)]^{\frac{1+v}{2}} \\ &\leq \gamma_1 V(t)^{\frac{1+v}{2}} \quad (30) \end{aligned}$$

where $\gamma_1 = a_{max}^v \bar{r}(N)^{\frac{1-v}{2}}$, a_{max} denote the maximum of a_{kj}^c, $\bar{r} = \max_{c=1,..,N}[N - (r_c - r_{c-1})]$ and r_c denote any particular agent in c^{th} microgrid. A similar analysis for V_4 & V_5 can be carried out using (27) & (30) respectively to get:

$$V_4(t) = -\Gamma_2 V(t)^{\frac{1+w}{2}}, V_5(t) = \gamma_2 V(t)^{\frac{1+w}{2}} \quad (31)$$

where $\Gamma_2 = \alpha 2^w \rho^{\frac{1+w}{2}}$ & $\gamma_2 = a_{max}^w \bar{r}(N)^{\frac{1-w}{2}}$. Summing up (25), (27), (30) & (31), we get:

$$\dot{V}(t) \leq 2\sigma V(t) - (\Gamma_1 - \gamma_1)V(t)^{\frac{1+v}{2}} - (\Gamma_2 - \gamma_2)V(t)^{\frac{1+w}{2}} \quad (32)$$

Using Theorem 1 [21], (32) can be simplified as:

$$\dot{V}(t) \leq \begin{cases} -(\Gamma_1 - \gamma_1 - 2\sigma)V(t)^{\frac{1+v}{2}}; & V(t) < 1 \\ -(\Gamma_2 - \gamma_2 - 2\sigma)V(t)^{\frac{1+w}{2}}; & V(t) \geq 1 \end{cases} \quad (33)$$

such that there exists a upper bound for fixed time T^*. Since (32) is independent of the initial value $V(0)$ as opposed to the finite-time strategies, fixed-time convergence holds true provided:

$$T^* = \int_0^\infty \frac{1}{f(V)dV} \quad (34)$$

is fixed. This completes the proof that fixed-time convergence of global as well as local objectives is ensured for DC microgrid clusters, without depending on initial operating values unlike [4]. However, the abovementioned analysis doesn't regard communication delay inherited in the cyber channels. It may lead to instability if the delay is significantly high. To determine the stability margin under such conditions, a time-delay analysis is carried out to determine the upper bound of communication delay that the system can withstand.

Time delay can occur due to multiple factors: jamming, traffic of signals, sequencing of packets resulting in packet loss. Such delays can have a major impact in control of networked microgrids, ultimately leading to divergent solutions [20]. Since time delays beyond a certain value affect the stability of the system, an upper bound of the delay margin needs to be investigated. In order to assess system stability under different time delays, a Lyapunov candidate function using Lyapunov-Krasovskii function approach [22], [23] is used for the delayed measurements in an infinite dimensional

space Υ. This space contains all the solution for x in the interval [t-τ, t] and can be represented as:

$$V(\Upsilon) = V_0(x(t)) + \int_0^{\tau_m} V_1(\tau, x(t), x(t-\tau))d\tau \quad (35)$$

where τ and τ_m denote communication delay and upper bound on communication delay respectively. Using (23), it can be established that the Lyapunov function is positive-definite. Since negative-definiteness/semi-definiteness of the time-delayed Lyapunov candidate is also required to prove stability, it is carried out using:

$$\dot{V}_f = \frac{1}{\tau_m}\dot{V} + \frac{1}{\tau_m}[V_1(\tau_m, x(t), x(t-\tau_m)) - V_1(0, x(0), x(t))] + \frac{\partial V_1}{\partial x(t)} - \frac{\partial V_1}{\partial \tau} \leq 0 \ \forall x(t), \forall x(t-\tau) \quad (36)$$

$\forall \tau \in [0, \tau_m]$. Additionally, since $V^{\frac{1+v}{2}} < V^2$, (36) can be alternatively written as:

$$\dot{V}_f \leq \frac{1}{\tau_m}\dot{V}(t) + \frac{1}{\tau_m}V^2(t-\tau_m) - \frac{1}{\tau_m}V^2(t) + 2V\dot{V} \quad (37)$$

Using (33), (37) can be further written as:

$$\dot{V}_f \leq -\underbrace{[\frac{1}{\tau_m} + 2V](\Gamma_1 - \gamma_1 - 2\sigma)V(t)^{\frac{1+v}{2}}}_{\iota} + \frac{1}{\tau_m}\omega \leq 0 \quad (38)$$

where $\omega = V^2(t-\tau) - V^2(t)$. Since all the terms in ι is positive using (27-(33), a necessary and sufficient criteria to achieve stability under time delay is by obtaining a negative-definite solution for (38), which provides a minimum value of ω equal to $\iota\tau_m$. Hence, for different values of maximum allowable communication delay τ_m, the stability of the cluster with time-delayed measurements can be assessed using the abovementioned criteria.

V. Simulation Results

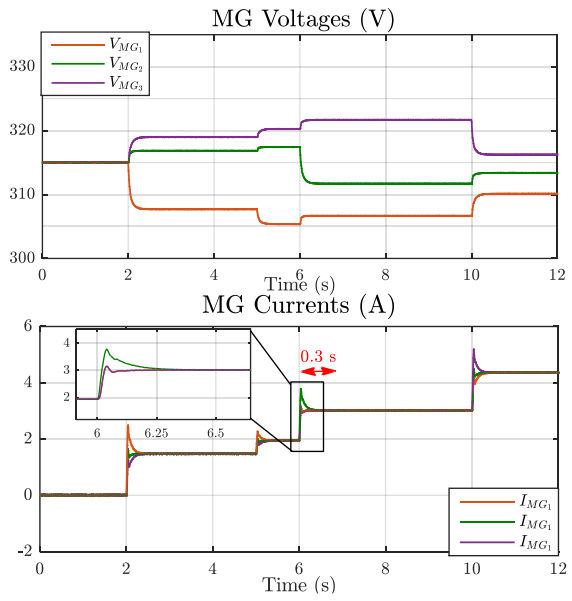

Fig. 6. Performance evaluation of loading mismatch mitigation using the proposed fixed-time based secondary controller: Faster settling time as compared to Fig. 2.

The proposed fixed-time cooperative secondary control strategy is tested on a DC microgrid cluster, as shown in Fig. 1, of rated voltage of 315 V with M = 3 microgrids of equal capacity of 10 kW are interconnected to each other via variable resistive feeder lines R_{cm}. Further, c^{th} microgrid consists of N = 3 BESSs, each of equal capacity of 1.6 kW, PV of 5.2 kW and resistive loads are connected to each other via variable resistive lines r^c_{kj} as shown in Fig. 1. It should be noted that equal capacity of BESS units in each microgrid has been considered for better understanding. Various load changes, insolation change scenarios have been considered in the local & global network to test the performance of the proposed fixed-time strategy. Furthermore, a control area network (CAN) bus model is designed for both cyber layers to realize the impact of communication delays and data packet loss. The global & local cyber layers are sampled at a frequency of 150 & 500 Hz respectively. Further, the plug-and-play capability of the proposed cooperative controller along with link failure resiliency and its impact on individual microgrids is studied in the global network. All the scenarios have been discussed in MATLAB/SIMULINK environment. The simulated system & control parameters are provided in Appendix A.

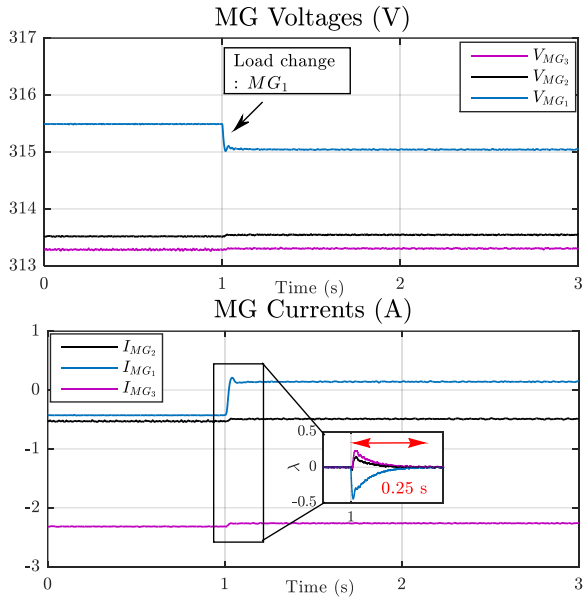

Fig. 7. Performance of the cluster prior to cooperative fixed-time based loss minimization strategy: Convergence in 0.25 s.

In Fig. 6, the loading mismatch mitigation between microgrids using the proposed control strategy is performed for the same loading condition and disturbances in Fig. 2. It can be seen that the performance of the proposed strategy during frequent load changes, I_{MG_c} in (6) is mitigating the loading mismatch between each microgrid in a significantly faster manner, i.e., 0.3 s as compared to asymptotic convergence in 3.4 s using [13], as shown in Fig. 2.

In Fig. 7, the performance of the online distributed loss minimization strategy is tested during light load conditions. As seen in Fig. 7 before t = 1 s, since the microgrid currents are negative, PV generation is more than the load, which suggests that BESSs are being charged. For an increase in load at t =

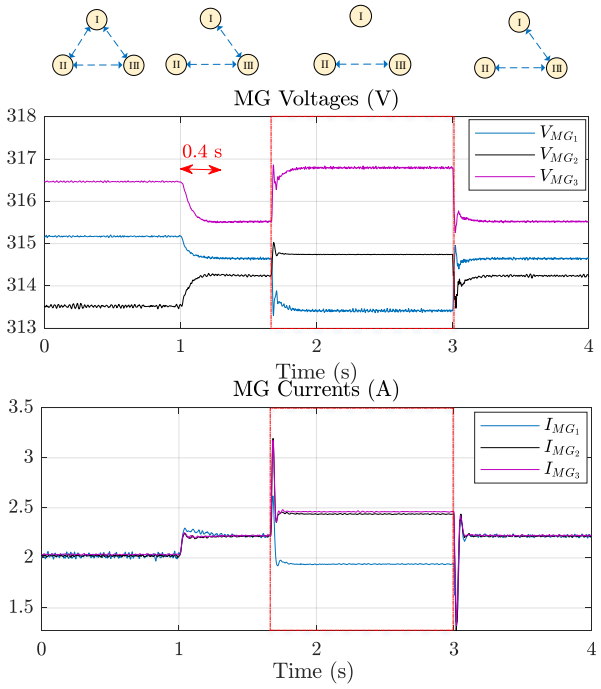

Fig. 8. Performance of the cluster during global layer link failure.

1 s in microgrid I(MG_1) in Fig. 1, the loading mismatch is mitigated in a disproportionate manner since the contribution of load current from MG_1 is quite high as compared to the rest of microgrids. As the load change is primarily met locally using the proposed strategy avoiding a flow of current via the feeders from other microgrids, the system efficiency is improved considering the high efficiency of individual converters during light load conditions. It can be seen in Fig. 7 that λ_c for each microgrid remarkably converges to zero using the proposed fixed-time convergence law in 0.25 s. Importantly, it operates as a secondary controller by handling the load changes online only using neighboring measurements making it a reliable approach for efficient operation of the cluster as compared to centralized communication.

All the analyses carried out after this point have been carried out with ϕ = 1 to demonstrate the performance of fixed-time based loading mismatch mitigation in the cluster.

Further, the robustness of the proposed controller against link failure resiliency in global as well as the local layer is verified. Firstly, link failure between microgrid agents is tested by disabling link I-II at t = 0.8 s in Fig. 8. However, the system responds by performing normally owing to the spanning tree nature of the global cyber network. However, when the link between I-III is lost at t = 1.75 s, the spanning tree connectivity of the cluster is lost, which rules out MG_1 in obeying global control objectives. Additionally since the link between II-III is still active, the corresponding MGs cater to mitigate the loading mismatch between them. Consequently, local agents in MG_1 resort back to achieve local secondary objectives to share local load current until t = 3 s where the link between I-III is set active. Upon restoration, it can be seen in Fig. 8 that each MG start mitigating the loading mismatch in the cluster. Moreover, the convergence owing to the proposed fixed-time consensus law is considerably faster as the voltage settles down within 0.4 s as compared to the conventional approach. Similarly in Fig. 9, the link

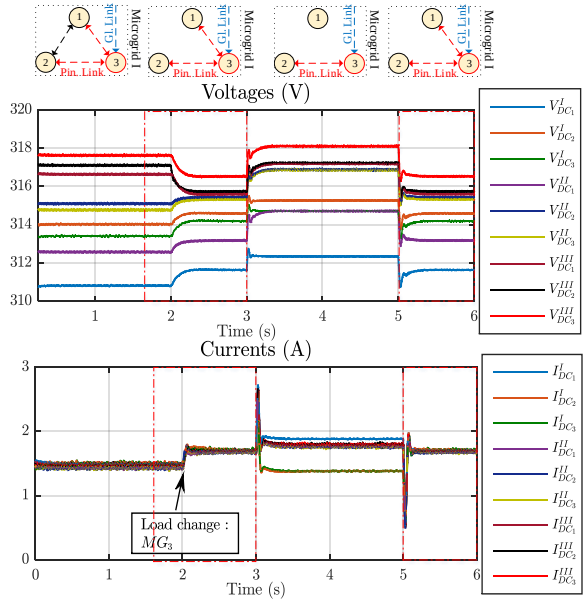

Fig. 9. Performance during local layer link failure in microgrid I.

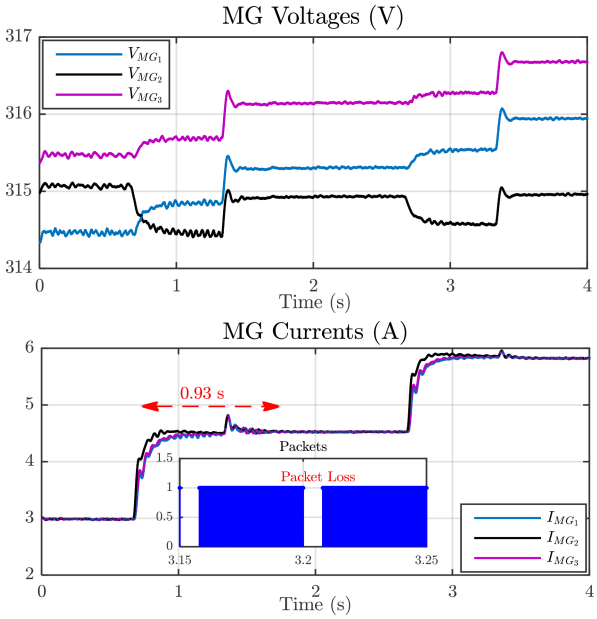

Fig. 10. Performance of the cluster for a maximum communication delay of 350 ms with 10% data packet loss every 50 ms

failure resiliency between the microgrid agent and the pinned agents in MG_1 is studied to supervise the local secondary objectives in each microgrid. At t = 0.8 s, when the local link between $BESS_1^1$ & $BESS_2^1$ is lost as highlighted in Fig. 9, it still manages to mitigate the loading mismatch which justifies link failure resiliency in the local distributed cyber layer since the spanning tree holds true for the local layer. Further, when the pinning link between $BESS_1^1$ & $BESS_3^1$ is lost, it disregards proportionate sharing. However, when

the link between $BESS_1^1$ & $BESS_3^1$ is re-activated at t = 5 s, which completes the spanning graph, the global as well as local secondary objectives are satisfactorily met. Fig. 10 shows the system performance under communication delay & data packet loss in the global layer. These disturbances have been modeled in MATLAB/SIMULINK environment using *FIFO Queue* in the CAN protocol which can be used to limit the number of packets buffered per interval. In Fig. 10, a maximum communication delay of 350 ms along with 10 % packet loss every 50 ms is introduced in every link of the global layer which yields a satisfactory performance with a settling time of 0.93 s. Hence, the performance of the proposed controller can be deemed satisfactory owing to the fixed-time convergence within 0.93 s based on the findings in [4] for maximum communication delays in different transmission medium.

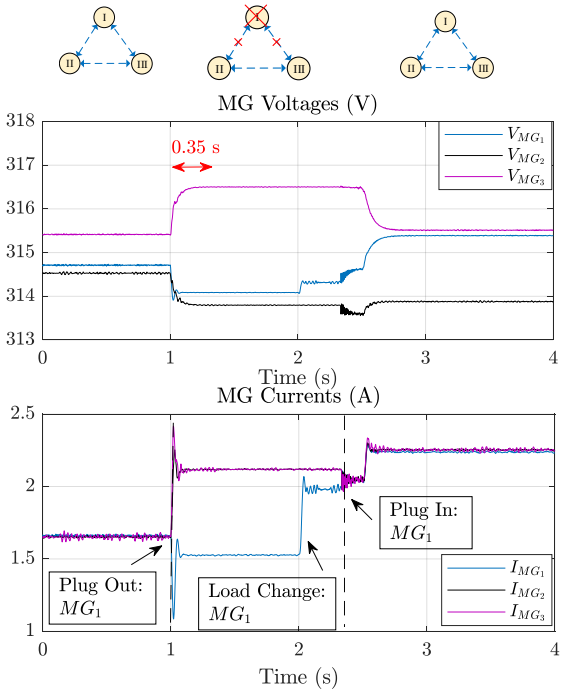

Fig. 11. Performance of the cluster for plug-and-play capability of a microgrid.

In Fig. 11, the plug-and-play capability of the proposed controller is validated by plugging in and out of MG_1 at t = 1 and t = 2.33 s respectively. With the outage of MG_1 at t = 1 s as highlighted in Fig. 11, each BESS in MG_2 & MG_3 share the remaining loads in the cluster since MG_1 is physically disconnected from the cluster. As a result, the local secondary controller in MG_1 using the local layer operates to share the local loads as MG_1 current drops to 1.5 A. When MG_1 is plugged back into the cluster at t = 2.33 s, each MG revert to mitigate loading mismatch as shown in Fig. 11.

VI. Conclusion

This paper proposes a dual layer fully distributed fixed-time based secondary controller, which achieves inter-microgrid & intra-microgrid objectives ensuring fixed-time convergence in a cluster of DC microgrids. As the conventional distributed approaches entail asymptotic convergence; they have adverse effects on network performance. To address this issue, a fixed-time consensus law based secondary approach is designed in this paper which facilitates fixed-time settling of objectives namely, loading mismatch mitigation in the global level and proportionate load current sharing, average voltage regulation locally in each microgrid. However, loading mismatch mitigation involves significant transmission line losses during light load conditions. To enhance system efficiency during light load conditions, a fixed-time based distributed loss minimization strategy is designed to operate as a secondary controller using online measurements from the neighboring microgrids. This concept improves the reliability as compared to the conventional tertiary approaches realized in a centralized fashion. Since fixed-time consensus is independent of the initial operating values, which is unknown for a large system, the proposed strategy can be readily implemented in practice. The simulation results demonstrate stable dynamic performance in case of physical disturbances such as plug out of converters as well as cyber intricacies such as variable communication delay and data packet loss. As a result, it facilitates the use of low-cost communication protocol.

Appendix A
Simulation Parameters

It should be noted that the values of variables without any subscript/superscript are consistent throughout the cluster.
Plant: R_{12} = 1.3 Ω, R_{13} = 1.8 Ω, R_{23} = 1.2 Ω, r_{23}^1 = 0.25 Ω, r_{13}^1 = 0.3 Ω, r_{12}^1 = 0.35 Ω, r_{1p}^1 = 0.2 Ω, r_{23}^2 = 0.15 Ω, r_{13}^2 = 0.2 Ω, r_{12}^2 = 0.4 Ω, r_{1p}^2 = 0.3 Ω, r_{23}^3 = 0.35 Ω, r_{13}^3 = 0.3 Ω, r_{12}^3 = 0.5 Ω, r_{1p}^3 = 0.1 Ω
Converter: L_i= 3 mH, C_{dc_i}= 250 μF
Controller: $R_{vir}^1 = R_{vir}^2 = R_{vir}^3$ = 0.8, α = 7.5, β = 4.5, d = 0.75, v = 0.5, w = 0.5

Appendix B
Design Guidelines Considering Communication Sampling Rate

To realize the control design guidelines for different communication sampling rate, the Lyapunov function in (23) is discretized to get

$$V_t = \frac{1}{2}\sum_{c=1}^{M}\sum_{k=1}^{N} P E_t^T E_t \tag{39}$$

at time instant t. Considering the difference between two samples for different communication rates along the trajectory for (39), we get

$$\Delta V_t = V_{t+1} - V_t = \frac{1}{2}\sum_{c=1}^{M}\sum_{k=1}^{N}(E_t^T)P(E_t^T)^T \tag{40}$$

for a positive matrix $P = diag\{(1+\frac{1}{\zeta})G, ..., (1+\frac{1}{\zeta_c})L_c\}, \{\zeta, ..., \zeta_c\} > 0$ using (1) & (2) where ζ used with subscript c corresponds to the local cyber layer in c^{th} microgrid whereas ζ denotes for the global cyber layer for the cluster. Hence, the design of the control gains can given by

achieving a sufficient condition for $\Delta V_t < 0$ using the special matrix theory and properties of symmetric graphs [24], given by

$$(1 + \frac{1}{\zeta})\rho(G) < 1 \tag{41}$$

$$(1 + \frac{1}{\zeta_c})\rho(L_c) < 1, \forall\ c\ \epsilon\ M \tag{42}$$

where ρ suggest the eigenvalues of the cyber graph which lie between origin and unit plane.

REFERENCES

[1] N. Hatziargyriou and H. Asano, R. Iravani and C. Marnay, "Microgrids," in *IEEE Power and Energy Magazine*, vol. 5, no. 4, pp. 54–65, 2007.

[2] Y. K. Chen, Y. C. Wu, C. C. Song, and Y. S. Chen, "Design and implementation of energy management system with fuzzy control for DC microgrid systems," *IEEE Trans. Power Electr.*, vol. 28, no. 4, pp. 1563–1570, 2013.

[3] T. Dragičević, X. Lu, J. C. Vasquez, and J. M. Guerrero, "DC Microgrids – Part I: A Review of Control Strategies and Stabilization Techniques", *IEEE Trans. Power Elect.*, vol. 31, no. 7, pp.4876–4891, 2016.

[4] S Sahoo, and S Mishra, "A Distributed Finite-Time Secondary Average Voltage Regulation and Current Sharing Controller for DC Microgrids." *IEEE Trans. on Smart Grid*, vol. 10, no. 1, pp. 282-292, 2019.

[5] E Rodriguez-Diaz, et al. "Multi-level energy management and optimal control of a residential DC microgrid." *Consumer Electronics (ICCE), 2017 IEEE International Conference on*, 2017.

[6] T. Dragičević, X. Lu, J. C. Vasquez, and J. M. Guerrero, "DC Microgrids–Part II: A Review of Power Architectures, Applications, and Standardization Issues," *IEEE Trans. Power Elect.*, vol. 31, no. 5, pp.3528–3549, 2016.

[7] SK Sahoo, AK Sinha, and NK Kishore, "Control Techniques in AC, DC, and Hybrid AC–DC Microgrid: A Review",*IEEE Journal of Emerg. And Select. Topics in Power Elect.*, vol. 6, no. 2, pp. 738–759, 2018.

[8] KT Tan, XY Peng, PL So, YC Chu and MZQ Chen, "Centralized control for parallel operation of distributed generation inverters in microgrids," *IEEE Trans. Smart Grid*, vol. 3, no. 4, pp. 1977–1987, 2012.

[9] S Sahoo, and S Mishra. "A Multi-Objective Adaptive Control Framework in Autonomous DC Microgrid", *IEEE Trans. Smart Grid*, vol. 9, no. 5, pp. 4918–4929, 2018.

[10] L. Meng, T. Dragičević, J Roldan-Perez, J. C. Vasquez and J. M. Guerrero, "Modeling and sensitivity study of consensus algorithm-based distributed hierarchical control for dc microgrids." *IEEE Trans. Smart Grid*, vol. 7, no. 3, pp. 1504–1515, 2016.

[11] V. Nasirian, S. Moayedi, A Davoudi and F. L. Lewis "Distributed Cooperative Control of DC Microgrids," *IEEE Trans. Power Elect.*, vol. 30, no. 4, pp. 2288–2303, 2015.

[12] S Anand, BG Fernandes, and JM Guerrero, "Distributed control to ensure proportional load sharing and improve voltage regulation in low-voltage DC microgrids" *IEEE Trans. Power Elect.*, vol. 28, no. 4, pp. 1900–1913, 2013.

[13] S Moayedi, and A Davoudi. "Distributed tertiary control of DC microgrid clusters." *IEEE Trans. Power Elect.*, vol. 31, no. 2, pp.1717-1733, 2016.

[14] Y Han, et al. "MAS-based Distributed Coordinated Control and Optimization in Microgrid and Microgrid Clusters: A Comprehensive Overview," *IEEE Trans. Power Elect.*, 2017.

[15] R Zhang and B Hredzak, "Distributed Finite-Time Multi-Agent Control for DC Microgrids with Time Delays", *IEEE Trans. on Smart Grid*, 2018.

[16] F Chen et al., "Analysis and distributed control of power flow in DC microgrids to improve system efficiency", *Envir. Friendly Energies and Appl. (EFEA), 2016 4th International Symposium on*, 2016.

[17] D. Maksimovic and I. Cohen, "Efficiency optimization in digitally controlled flyback DC–DC converters over wide ranges of operating conditions," *IEEE Trans. Power Electron.*, vol. 27, no. 8, pp. 3734–3748, Aug. 2012.

[18] T. Dragičević, J. M. Guerrero, J. C. Vasquez and D. Skrlec, "Supervisory control of an adaptive-droop regulated DC microgrid with battery management capability," *IEEE Trans. Power Elect.*, vol. 29, no. 2, pp. 695–706, 2015.

[19] L Meng et al. "Tertiary and Secondary Control Levels for Efficiency Optimization and System Damping in Droop Controlled DC–DC Converters", *IEEE Trans. Smart Grid*, vol. 6, no. 6, pp. 2615-2626, 2015.

[20] S Sahoo, et. al. "A Cooperative Adaptive Droop Based Energy Management & Optimal Voltage Regulation Scheme for DC Microgrids", *IEEE Trans. Ind. Elect.*, pp. 1-1, 2019.

[21] W. L. Lu, X. W. Liu, and T. P. Chen, "A note on finite-time and fixed-time stability," *Neural Netw.*, vol. 81, pp. 11–15, Sep. 2016.

[22] A Papachristodoulou, MM Peet, and S Lall, "Analysis of Polynomial Systems With Time Delays via the Sum of Squares Decomposition", *IEEE Trans. Autom. Control*, vol. 54, no. 5, pp. 1058-1064, May 2009.

[23] S Sahoo, et. al, "A containment based distributed finite-time controller for bounded voltage regulation & proportionate current sharing in DC microgrids", *Applied Energy*, vol. 228, pp. 2526-2538, 2018.

[24] R. Horn, and C. Jornson, "Matrix Analysis", New York, Cambridge University Press, 1985

Subham Sahoo (S'16-M'18) received the B.Tech. & Ph.D. degree in Electrical and Electronics Engineering from VSS University of Technology, Burla, India and Electrical Engineering at Indian Institute of Technology, Delhi, New Delhi, India in 2014 & 2018 respectively. He has worked as a visiting student with the Department of Electrical and Electronics Engineering in Cardiff University, UK in 2017 and as a postdoctoral researcher in the Department of Electrical and Computer Engineering in National University of Singapore in 2018-2019. He is currently working as a research fellow in the Department of Energy Technology, Aalborg University, Denmark.

His current research interests include microgrids, cyber security, control and stability of cyber-physical systems.

Sukumar Mishra (M'97-SM'04) is a Professor at Indian Institute of Technology, New Delhi and has been part of IIT Delhi for the past 15 years. He has published over 200 research articles (including papers in international journals, conferences and book chapters).

Prof. Mishra has won many accolades throughout his academic tenure of 25 years. He has been a recipient of INSA medal for young scientist (2002), INAE young engineer award (2009), INAE silver jubilee young engineer award (2012) and has recently won the Samanta Chandra Shekhar Award (2016). He has been granted fellowship from many prestigious technical societies like IET (UK), NASI (India), INAE (India), IETE (India) and IE (India) and is also recognized as the INAE Industry Academic Distinguish Professor. Apart from all research and academic collaborations, Prof. Mishra is very actively involved in industrial collaborations. Prof. Mishra is currently acting as NTPC Chair professor and has previously delegated as the Power Grid Chair professor. He is also serving as an Independent Director of the Cross Border Power Transmission Company Ltd. and the River Engineering Pvt. Ltd. Prof. Mishra has also carried out many important industrial consultations with TATA Power, Microtek and others. Prof. Mishra's research expertise lies in the field of Power Systems, Power Quality Studies, Renewable Energy and Smart Grid. He is currently serving as an Editor for the IEEE Transactions on Smart Grid, IEEE Transactions on Sustainable Energy and an Associate Editor for the IET Generation, Transmission & Distribution journal.

Seyed Mahdi Fazeli received the Ph.D. degree from the University of Malaya, Kuala Lumpur, Malaysia, in 2013. He is currently working as Researcher with the Centre for Sustainable Power Distribution, University of Bath, Bath, U.K.

His main research interests include power electronic, variable-speed ac drives, HVDC system, flexible ac transmission system (FACTS), and nonlinear control. He is a member of the Institution of Engineering and Technology and a Chartered Engineer.

Furong Li (SM'09) was born in Shannxi province, China. She received the B.Eng. degree in electrical engineering from Hohai University, Nanjing, China, in 1990 and the Ph.D. degree from Liverpool John Moores University, Liverpool, U.K., in 1997.

She is a professor in the Power and Energy Systems Group, University of Bath. Her major research interest is in the area of power system planning, analysis, and power system economics.

Tomislav Dragičević (S'09-M'13-SM'17) received the M.Sc. and the industrial Ph.D. degrees in Electrical Engineering from the Faculty of Electrical Engineering, Zagreb, Croatia, in 2009 and 2013, respectively. From 2013 until 2016 he has been a Postdoctoral research associate at Aalborg University, Denmark. From March 2016, he is an Associate Professor at Aalborg University, Denmark where he leads an Advanced Control Lab.

He made a guest professor stay at Nottingham University, UK during spring/summer of 2018. His principal field of interest is design and control of microgrids, and application of advanced modeling and control concepts to power electronic systems. He has authored and co-authored more than 170 technical papers (more than 70 of them are published in international journals, mostly IEEE Transactions) in his domain of interest, 8 book chapters and a book in the field.

He serves as Associate Editor in the IEEE TRANSACTIONS ON INDUSTRIAL ELECTRONICS, in IEEE Emerging and Selected Topics in Power Electronics and in IEEE Industrial Electronics Magazine. Dr. Dragičević is a recipient of the Končar prize for the best industrial PhD thesis in Croatia, and a Robert Mayer Energy Conservation award.